Preparation and photocatalytic ability of highly defective carbon nanotubes

Yongsong Luo [a,c,*], Yaofu Heng [b], Xiaojun Dai [a], Wenquan Chen [a], Jialin Li [c]

[a] Department of Physics Electronic Engineering, Xinyang Normal University, Xinyang 464000, People's Republic of China
[b] Department of Electronic Science and Engineering, Huanghuai University, Zhumadian 463000, People's Republic of China
[c] Department of Physics, Central China Normal University, Wuhan 430079, People's Republic of China

ARTICLE INFO

ABSTRACT

The highly defective carbon nanotubes (CNTs) were prepared using a heat-treatment technique and their photocatalytic ability was reported for the first time. The results showed that the highly defective CNTs had the photocatalytic ability in the range of visible light. The results also indicated that the electrical properties of CNTs were dependent not only on the diameter and helicity but also on the defect number of tubes. The defects of CNTs might be produced from vacancies, local lattice reordering and intertube reorientation during the course of the desorption of oxygen atoms, which could initiate defect states in the band gap. Absorption of visible light led to the formation of electron/hole pairs and hence caused photocatalytic oxidation. Consequently, the highly defective CNTs having the photocatalytic ability would be promising as a new photocatalytic material in the visible light.

1. Introduction

Carbon nanotubes (CNTs) are a class of nanomaterials with interesting electrical and mechanical properties that make them potential candidates for electronic devices. Though the properties of the atomically perfect CNTs have been understood relatively well, experimental and theoretical calculations have shown that structural defects in CNTs, such as topological defects, vacancies, and chemical modifications, can substantially modify their electronic properties [1–3], thermal conductivity [4,5] and phonon transport [6,7]. Recently, with improvement of experimental techniques, direct observation of the atomic-scale defects in graphene layers has enabled us to investigate the physical and chemical properties of defective carbon nanostructures in detail [8–13]. For example, Gomez-Navarro et al. showed that even a low concentration of vacancies in CNTs can produce a large decrease in their electrical conductance [11]. Introducing a stone-wales defect into the CNTs can further decrease the band gap compared to the case of perfect tube under the same deformation in Fa's research group [14]. An electrochemical process developed by Fan et al. [12] for controlling the defects makes the design of reliable CNT electronic circuits possible. On the other hand, the presence of defects can also introduce new functions like chemical response and electrocatalysis to the CNTs [15,16].

Since the defects have a significant influence on the electronic and mechanical properties of CNTs [17–19], some researchers have artificially introduced the defects on the surfaces of CNTs by purification treatment or irradiation with charged particles [20,21]. Zhu et al. pointed out that energetic Ar^+ ion could produce dangling bonds (vacancies) on the surface of nanotubes [20]. Osvath et al. reported the atomic-scale CNTs defects produced by Ar^+ ion irradiation [21]. In this paper, we prepared the highly defective CNTs with a heat-treatment technique and studied their photocatalytic ability. Usage of photocatalytic degradation of H_2O_2 is one effective, reliable and easily detective method for investigating photocatalytic ability of highly defective CNTs, which needs relatively low free energy. The results displayed that the highly defective CNTs showed the photocatalytic ability. To the best of our knowledge, the photocatalytic ability of highly defective CNTs has not been reported so far.

2. Experimental

In this work, CNTs were grown at low temperatures (700 °C) using the thermal chemical vapor deposition (CVD) method. A Fe-coated Al substrate was used for the CNTs deposition [22]. The raw CNTs were purified with the mixed acid of HNO_3 (45 vol%), HCl (45 vol%), HF (10 vol%) and residues including metal particles, amorphous carbon, carbon nanoparticles, graphite, etc. were removed [23–25]. These purified CNTs are denoted as functionalized CNTs (F-CNTs). Subsequently, the F-CNTs were rinsed with de-ionized water thoroughly, dried, milled and annealed at 1200 °C under high vacuum (10^{-4} Pa) for 2 h, the

* Corresponding author at: Department of Physics Electronic Engineering, Xinyang Normal University, Xinyang 464000, People's Republic of China. Fax: +86 376 6391705.
  E-mail addresses: ysluo@mail2.xytc.edu.cn (Y. Luo), lijl@phy.ccnu.edu.cn (J. Li).

final products are the highly defective CNTs (which are also referred to defunctionalized CNTs (DF-CNTs)). Moreover, high temperature CNTs (820 °C) were also prepared under the same condition, these purified (functionalized) and defunctionalized CNTs are named as FH-CNTs and DFH-CNTs, respectively.

The photocatalytic experiment was carried out with the equipment of photocatalysis (i.d. 8 cm) of 500 ml capacity. The equipment of photocatalysis consists of a three-layer tube-shaped terrarium. The reactants were irradiated using a 500 W tube-shaped tungsten lamp from the hollow of the reactor. The outer thimble is reactor and the inner is connected to cooling water, and the reaction temperature was maintained at ambient temperature by passing water through the inner thimble. Further water passed through the inner thimble of the reactor, therefore the temperature of the reaction mixtures would be kept at 30 °C. In the photocatalytic experiment, the highly defective CNTs were used as the photocatalyst, the equilibrated adsorption of solution on the highly defective CNTs was performed with stirring for 12 h in the dark before exposing the reactor assembly to the concentrated tube-shaped tungsten lamp. A sample was taken for analysis in definite time interval. The concentration of H_2O_2 in this filtered sample was treated as the zero time concentration in each experiment before exposure to radiation, presaturated air was bubbled at sufficiently high velocity ($2.5 \, cm \, s^{-1}$) to keep all the highly defective CNTs in suspension. Moreover, the presaturated air was also used as an electron scavenger.

Hydrogen peroxide concentrations were determined by iodide method ($\lambda_{max} = 352 \, nm$) [26]. The iodide method (detection limit of $\approx 10^{-6} \, M$) allows one to distinguish between H_2O_2 and organic peroxides since the latter reacts more slowly with the molybdenum–iodide system. Aliquots (1.5 ml) of CNTs suspensions were filtered, and then 0.75 ml of 0.1 M potassium biphthalate was added. At $t = 0 \, min$, 0.75 ml of iodide reagent (0.4 M potassium iodide, 0.06 M NaOH, $\approx 10^{-4} \, M$ ammonium molybdate) was added, and the absorbance vs. time profile was recorded on a Shimadzu UV-2450 double-beam recording spectrophotometer. Moreover, RM-1000 confocal Raman microspectroscopy was used for Raman spectra analysis. SORPTOMAIC-1900 absorption device was used for BET analysis and PHI5300 X-ray photoelectronic spectroscopy was used for XPS analysis. Transmission electron microscopy (TEM) analysis was also carried out on an HRTEM JEM-2010FEF instrument (operated at 200 keV).

3. Results and discussion

Raman scattering has been used for many years as a probe of disorder in the carbon skeleton of sp^2 and sp^3 carbon materials [27], disorder in the graphene structure of the tube wall of CNTs leads to the appearance of a broad disorder band or D band [28–30]. The most important features are the disorder induced D band at 1320–1370 cm^{-1}, the relative intensity of this mode can provide direct evidence of covalent modification and defect concentration, its second harmonic G' (shoulder in G) at 1601–1612 cm^{-1}, and the tangential G band at 1530–1610 cm^{-1} which is related to the graphite tangential E_{2g} Raman active mode where the two atoms in graphene unit cell are vibrating tangentially one against the other. Second order weak bands also occur at 2682–2692 cm^{-1} (D^*) and 2914–3218 cm^{-1} ($D+G$). When estimating the defect concentration, the D mode intensity is usually normalized with respect to the intensity of the G mode; this approach relies on the assumption that the intensity of the G mode is independent of defect concentration and originates from a single resonant Raman process [31,32]. Furthermore, the D band is activated in the first order scattering process of sp^2 carbons by the presence of in plane substitutional heteroatom vacancies,

grain boundaries, or other defects and by finite size effects, all of which lower the crystalline symmetry of the quasiinfinite lattice. Therefore the D mode can be used as a diagnostic of disruptions in the hexagonal framework of CNTs and is induced by double resonance process [33]. Fig. 1 shows Raman spectra, acquired at 514.5 nm excitation, collected from F (a), DF (b), FH (c) and DFH (d) carbon nanotubes, respectively. The results show that the relative intensity of the D and G modes is different for different CNTs, which can be attributed to the variety of defect concentration. From Fig. 1(b), the D mode intensity of DF-CNTs is higher than the G mode; moreover, the full width half maximum (FWHM) of the D mode is apparently larger compared to other CNTs, which usually indicates that the DF-CNTs are highly defective.

Usually the I_D/I_G ratio is also taken as a measure of defect concentration. Moreover, in order to get reliable information about the defect density it is necessary to include the intensity of the second order overtone mode D^* (or I_{D^*}/I_G), which is due to two phonon processes and hence to first approximation independent of defect concentrations [31,34,35]. Fig. 2 displays the
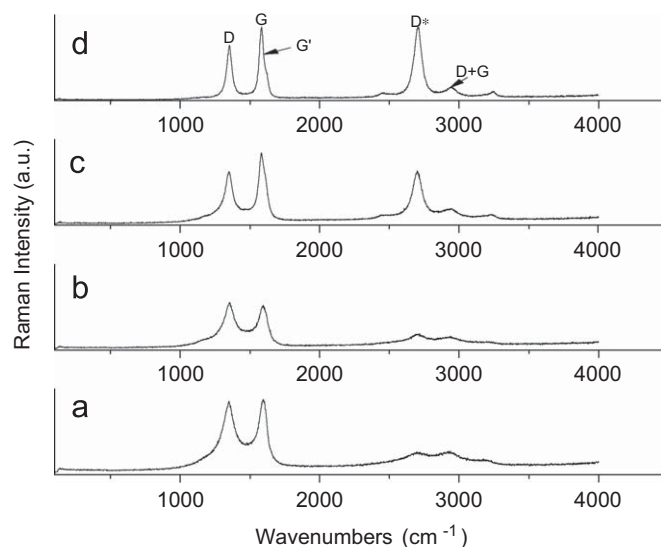

Fig. 1. Raman spectra at a laser of 514.5 nm excitation of F (a), DF (b), FH (c), and DFH (d) carbon nanotubes.
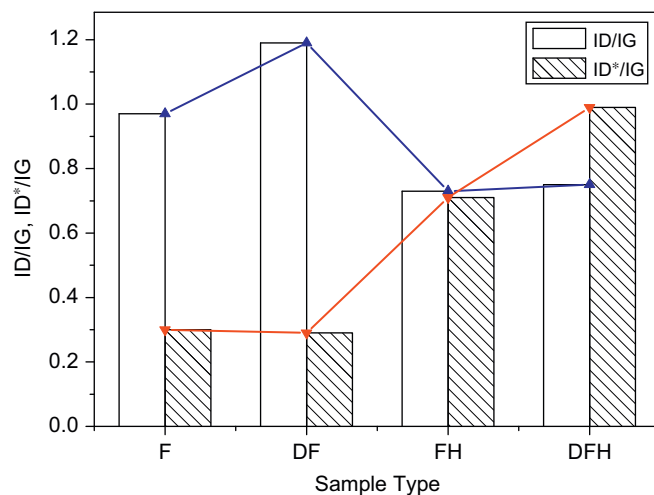

Fig. 2. Relative intensities: I_D/I_G and I_{D^*}/I_G of the Raman peaks for F, DF, FH, and DFH samples using a 514.5 nm excitation wavelength.
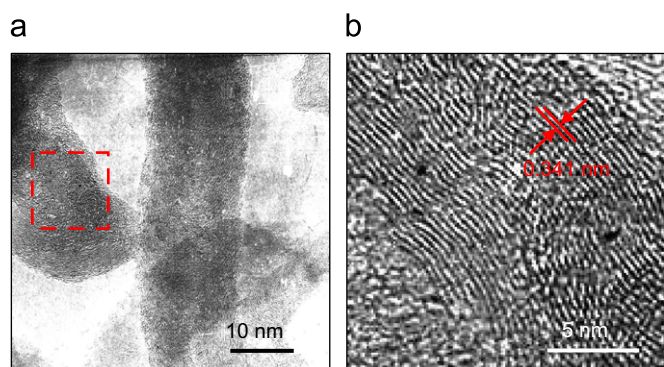
a

b

Fig. 3. (a) HRTEM image of an individual CNT and (b) enlarged image of the area marked by a rectangle in panel (a).

Table 1
Difference of CNTs multipoint specific surface areas (BET) in different phases.

Samples (sq m/g)	Raw	Purified (functionalized)	Annealed (defunctionalized)
CNTs (700 °C)	178.82	199.83	269.56
CNTs (820 °C)	87.68	116.60	131.62

corresponding ratios using the relative intensity of the peaks. It is clear that the DF-CNTs have the largest defect density in terms of the values of the I_D/I_G ratio (I_D/I_G = 1.19). The contrary trend is observed for I_{D^*}/I_G ratios, which further verified that the DF-CNTs are the highly defective nanotubes.

The defects of the DF-CNTs structures were further investigated by HRTEM. Fig. 3a shows the HRTEM image of an individual CNT. From this image, it can be seen that the CNT diameter is about 15–20 nm. The enlarged image of the area labeled by a rectangle (Fig. 3a) further reveals that the CNT is highly defective, including the abundant mismatches and a lot of vacancies (Fig. 3b). Careful examination reveals that the interfacial lattice spacing of the MWNTs is 0.341 nm, a value similar to the layer spacing in graphite. Moreover, this result was also confirmed through the change of the specific surface areas (BET) (the DF-CNTs have the largest BET corresponding to others CNTs), as presented in Table 1.

Photocatalytic degradation experiments for H_2O_2 were conducted in the reactor assembly. H_2O_2 (50 ml 10 mM) feed was added directly to 450 ml aqueous solution, various H_2O_2 concentrations were obtained by the iodide method (λ_{max} = 352 nm). Each experiment was conducted for 3 h and samples were taken at 0, 10, 20, 30 min, and 1 h interval, the highly defective CNTs (DF-CNTs) loading is 0.5 g in 1 l of solution. Considering the relatively unstable molecule of H_2O_2 and the effect of other CNTs (including F-CNTs, FH-CNTs and DFH-CNTs), the corresponding control experiment was also carried out. As a result, the change in H_2O_2 concentration is almost zero for the case of no CNTs. Obviously, the presence of highly defective CNTs (DF-CNTs) has shown pronounced influence on the degradation of H_2O_2 (Fig. 4). Moreover, the above samples of highly defective CNTs were recycled for four times under the same condition, the results clearly indicate that the photocatalytic activity of highly defective CNTs is very stable and reproducible (Fig. 5).

It is well known that defect-free CNTs can be metallic, semimetallic, or semiconducting depending on their diameter and helicity [1,3,36]. However, introduction of defects can alter the electronic properties of CNTs drastically. In this work, the highly defective CNTs (DF-CNTs) were obtained by further purifying and annealing the as-prepared CNTs at a low-tempera-
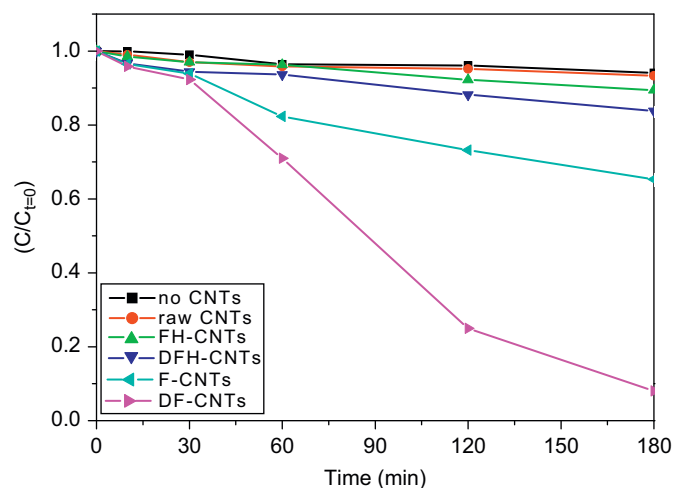

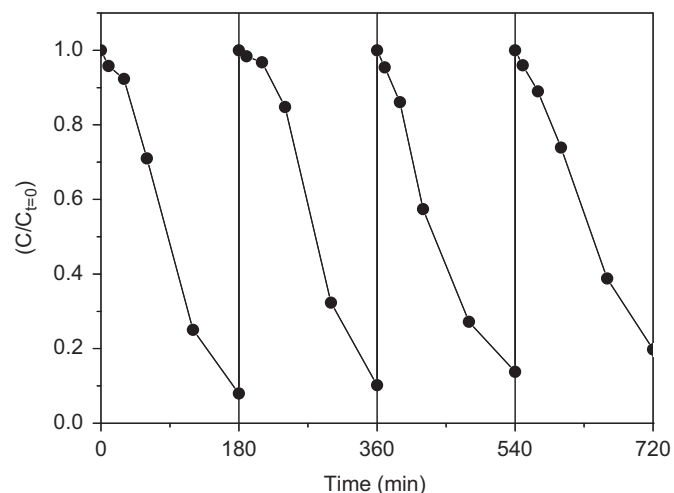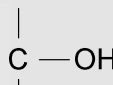**Fig. 4.** Effect of presence of different CNTs on potocatalytic degradation of H_2O_2.
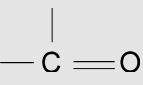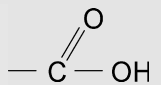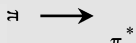

Fig. 5. Effect of photocatalytic degradation of H_2O_2 with the DF-CNTs during prolonged operation.

ture. In contrast to the high-temperature prepared CNTs, the low-temperature prepared CNTs have smaller diameter and contain more defects under the same synthetic condition. When they were purified by chemical oxidation, not only the new defects come forth on CNTs, but also the ends and often the sidewalls of the nanotubes are covered with a lot of oxygen-containing functional groups such as carboxylate and ether groups, which is named as F-CNTs. Then the F-CNTs were further annealed using the heat-treatment technique, most of chemisorbed oxygen would be desorbed and the oxygen atoms desorbed from the surfaces of CNTs through the formation of CO and CO_2 [37]. The oxygen release would cause the transformation of oxygen-containing functional groups (detailed in Table 2).

It is worth emphasizing that the desorbed oxygen gas induces a significant change in the geometric structures and electronic character of CNTs. In particular, the surface energy of CNTs would increase drastically, the individual CNTs were easily deformed and the intertube wall was facilely tangled. The deformed CNTs could result in two possible changes in the local structure of the tube: local lattice reordering and intertube reorientation [38]. The local lattice reordering will lead to the formation of topological defects. Moreover, the oxygen atoms desorbed from the surfaces of CNTs would also produce abundant vacant defects

Table 2
The XPS results of oxygen-containing functional groups for CNTs surface (700 °C).

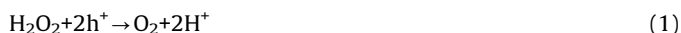| Groups	$-\overset{\textstyle\vert}{\underset{\textstyle\vert}{C}}-$		$\overset{\textstyle\vert}{\underset{\textstyle\vert}{C}}-OH$		$-\overset{\textstyle\vert}{C}=O$		$-\overset{\textstyle O}{\underset{\textstyle\ \ }{C}}-OH$		$\rightleftarrows \longrightarrow \pi^*$	
	B.E. (eV)	CON (%)	B.E. (eV)	CON (%)	B.E. (eV)	CON (%)	B.E. (eV)	CON (%)	B.E. (eV)	CON (%)
Raw CNTs	284.40	77.02	286.28	18.52	287.80	1.12	289.16	1.68	290.92	1.65
F-CNTs	284.40	73.98	286.28	19.38	287.80	1.07	289.16	3.15	290.92	2.43
DF-CNTs	284.40	74.02	286.28	19.21	287.80	1.64	289.16	2.48	290.92	2.65

B.E: binding energy (eV); CON: concentration %.
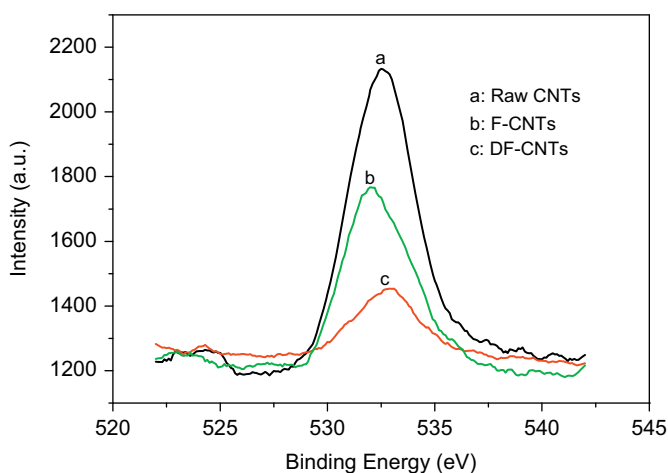
Fig. 6. O1s XPS spectra of raw CNTs, F-CNTs, and DF-CNTs.

on the surfaces of CNTs. As a result, this could initiate defect states in the band gap [39,40].

On the other hand, the intertube wall slippage during deformation could also change the interplayer interactions and result in the opening of a pseudogap [41]. Tekleab et al. [38] also testified that the mechanically deformed CNTs could yield a bandgap value of 0.20 ± 0.03 eV in the kink (defect). From XPS O1s spectrum of CNTs (Fig. 6), the highly defective CNTs clearly distinguish a greater symmetry through the heat-treatment (curve C); this effect can also be ascribed to an increased semiconductor behavior of highly defective CNTs [42].

Therefore, absorption of lights leads to formation of electron/hole pairs on the surfaces of the highly defective CNTs and causes degradation of H_2O_2, the detailed mechanisms are given as follows [43–45]:

$$H_2O_2 + 2h^+ \rightarrow O_2 + 2H^+ \tag{1}$$

$$H_2O_2 + h^+ \rightarrow HO_2^. + H^+ \tag{2}$$

$$H_2O_2 + e^- \rightarrow HO^. + OH^- \tag{3}$$

$$O_2 + e^- \rightarrow O_2^{-.} \tag{4}$$

$$H_2O_2 + O_2^{-.} \rightarrow HO^. + HO^- + O_2 \tag{5}$$

$$H_2O_2 + h\nu \rightarrow 2HO^. \tag{6}$$

$$HO^. + H_2O_2 \rightarrow HO_2^. + H_2O \tag{7}$$

On the other hand, H_2O_2 may also be photoproduced.

$$O_2 + e^- + 2H^+ \rightarrow H_2O_2 \tag{8}$$

$$HO_2^. + HO_2^. \rightarrow H_2O_2 + O_2 \tag{9}$$

$$HO_2^. + O_2^{-.} + H^+ \rightarrow H_2O_2 + O_2 \tag{10}$$

Herein, high concentrations of H_2O_2 are offered in the front of illumination, and the concentrations of photoproduced H_2O_2 are very low through redox of electron/hole pair. Therefore, it is well understood that the concentrations of H_2O_2 were reduced in the process of photocatalysis.

4. Conclusions

The present work has reported that the highly defective CNTs have the photocatalytic ability. The results indicated that photocatalytic degradation of H_2O_2 can be clearly observed with the highly defective CNTs in the visible light range. The DF-CNTs could present the relatively high surface energy which could then cause the change of the local structure of the tube, including local lattice reordering and intertube reorientation. The local lattice reordering would lead to the formation of more topological defects. At the same time, the oxygen atoms desorbed from the surfaces of CNTs would produce abundant vacant defects. These defects could initiate defect states in the band gap. Consequently, absorption of lights leads to formation of electron/hole pairs on the surface of the highly defective CNTs and then causes photocatalytic degradation of H_2O_2.

References

[1] N. Hamada, S. Sawada, A. Oshijama, Phys. Rev. Lett. 68 (1992) 1579.
[2] G.H. Lu, L.Y. Zhu, P.X. Wang, J.H. Chen, D.A. Dikin, R.S. Ruoff, Y. Yu, Z.F. Ren, J. Phys. Chem. C 111 (2007) 17919.
[3] J.W. Mintmire, B.I. Dunlop, C.T. White, Phys. Rev. Lett. 68 (1992) 631.
[4] T. Yamamoto, S. Watanabe, K. Watanabe, Phys. Rev. Lett. 92 (2004) 075502.
[5] N. Mingo, D.A. Broido, Phys. Rev. Lett. 95 (2005) 096105.
[6] C. Yu, L. Shi, Z. Yao, D. Li, A. Majumdar, Nano Lett. 5 (2005) 1842.
[7] H.Y. Chiu, V.V. Deshpande, H.W.C. Postma, C.N. Lau, C. Miko, L. Forro, M. Bockrath, Phys. Rev. Lett. 95 (2005) 226101.
[8] A. Hashimoto, K. Suenaga, K. Urita, S. Ijima, Nature 430 (2004) 870.
[9] K. Urita, K. Suenaga, T. Sugai, H. Shinohara, S. Iijima, Phys. Rev. Lett. 94 (2005) 155502.
[10] A.J. Lu, B.C. Pan, Phys. Rev. B. 71 (2005) 165416.
[11] C. Gomez-Navarro, P.J. De Pablo, J. Gomez-Herrero, B. Biel, F.J. Garcia-Vidal, A. Rubio, F. Flores, Nat. Mater. 4 (2005) 534.
[12] Y. Fan, N. Emmott, P.G. Collins, in: Technical Proceedings of the 2005 NSTI Nanotechnology Conference and Trade Show, vol. 2, 2005, p. 230.
[13] C.C. Tang, D. Golberg, Y. Bando, F.F. Xu, B.D. Liu, Chem. Commun. (2003) 3050.
[14] W. Fa, F.L. Hu, J.M. Dong, Phys. Lett. A 331 (2004) 99.
[15] J. Wang, Electroanalysis 17 (2005) 7.
[16] C.E. Banks, R.G. Compton, Analyst 131 (2006) 15.
[17] B.I. Yakobson, P. Avouris, Appl. Phys. 80 (2001) 287.
[18] J.C. Charlier, Acc. Chem. Res. 35 (2002) 1063.
[19] M.B. Nardelli, B.I. Yakobson, J. Bernholc, Phys. Rev. Lett. 81 (1998) 4656.
[20] Y.F. Zhu, T. Yi, B. Zheng, L.L. Cao, Appl. Surf. Sci. 137 (1999) 83.
[21] Z. Osvath, G. Vertesy, L. Tapaszto, F. Weber, Z.E. Horvath, J. Gyulai, L.P. Biro, Mater. Sci. Eng. C 26 (2006) 1194.
[22] E. Couteau, K. Hernadi, J.W. Seo, L. Thien-Nga, C. Miko, R. Gaal, L. Forro, Chem. Phys. Lett. 378 (2003) 9.
[23] F. Valentini, A. Amine, S. Orlanducci, M.L. Terranova, G. Palleschi, Anal. Chem. 75 (2003) 5413.
[24] Y.S. Park, Y.C. Choi, K.S. Kim, D.C. Chung, D.J. Bae, K.H. An, S.C. Lim, X.Y. Zhu, Y.H. Lee, Carbon 39 (2001) 655.
[25] J. Liu, A.G. Rinzler, H.J. Dai, J.H. Hafner, R.K. Bradley, P.J. Boul, A. Lu, T. Iverson, K. Shelimov, C.B. Huffman, F. Rodriguez-Macias, Y.S. Shon, T.R. Lee, D.T. Colbert, R.E. Smalley, Science 280 (1998) 1253.
[26] C. Kormann, D.W. Bahnemann, M.R. Hoffmann, Environ. Sci. Technol. 22 (1988) 798.
[27] J.P. Michael, Analytical Applications of Raman Spectroscopy [M], Blackwell Science, Cambridge, 1999.
[28] Y. Wang, D.C. Alsmeyer, R.L. McCreery, Chem. Mater. 2 (1990) 557.
[29] F. Tunistra, J.L. Koenig, Chem. Phys. 53 (1970) 1126.
[30] P.C. Eklund, J.M. Holden, R.A. Jishi, Carbon 33 (1995) 959.
[31] H. Murphy, P. Papakonstantinou, T.I.T. Okpalugo, J. Vac. Sci. Technol. B 24 (2006) 715.
[32] M.S. Dresselhaus, G. Dresselhaus, A. Jorio, A.G. Souza Filho, R. Saito, Carbon 40 (2002) 2043.
[33] S.R. Thomsen, J. Maultzsch, Philos. Trans. R. Soc. London Ser. A 362 (2004) 2337.
[34] J. Maultzsch, S. Reich, C. Thomsen, Appl. Phys. Lett. 81 (2002) 2647.
[35] U.J. Kim, C.A. Furtado, X. Liu, G. Chen, P.C. Eklund, J. Am. Chem. Soc. 127 (2005) 15437.
[36] R. Saito, M. Fujita, G. Dresselhause, M.S. Dresselhaus, Appl. Phys. Lett. 60 (1992) 2204.
[37] S.C. Lim, C.S. Jo, H.J. Jeong, Y.M. Shin, Y.H. Lee, I.A. Samayoa, J. Choi, Jpn. J. Appl. Phys. 41 (2002) 5635.
[38] D. Tekleab, R. Czerw, D.L. Carroll, Appl. Phys. Lett. 76 (2000) 3594.
[39] L. Chico, V.H. Crespi, L.X. Benedict, S.G. Louie, M.L. Cohen, Phys. Rev. Lett. 76 (1996) 971.
[40] M. Menon, D. Srivastava, Phys. Rev. Lett. 79 (1997) 4453.
[41] Y.K. Kwon, D. Tomanek, Phys. Rev. B. 58 (1998) 16001.
[42] G. Abstreiter, Light Scattering in Solids [M], Springer, Berlin, 1984.
[43] C.H. Liao, M.C. Lu, S.H. Su, Chemosphere 44 (2001) 913.
[44] D.D. Dionysios, M.T. Suidan, E. Bekou, I. Baudin, J.M. Laine, Appl. Catal. B Environ. 26 (2000) 153.
[45] B. Ahmmad, Y. Kusumoto, S. Somekawa, M. Ikeda, Catal. Commun. 9 (2008) 1410.